

Sulfamoylbenzamide-based Capsid Assembly Modulators for Selective Inhibition of Hepatitis B Viral Replication

Yeon Hee Lee,[▽] Hyeon-Min Cha,[▽] Jun Yeon Hwang, So Yeong Park, Avinash G. Vishakantegowda, Ali Imran, Joo-Youn Lee, Yoon-Sun Yi, Sangmi Jun, Ga Hyeon Kim, Hyo Jin Kang, Sang J. Chung, Meehyein Kim, Hyejin Kim,* and Soo Bong Han*Cite This: *ACS Med. Chem. Lett.* 2021, 12, 242–248

Read Online

ACCESS |

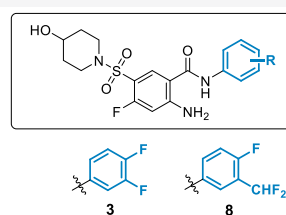
Metrics & More

Article Recommendations

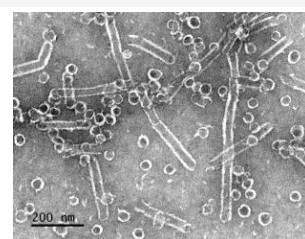
Supporting Information

ABSTRACT: As the spread of infections caused by hepatitis B virus (HBV) threatens public health worldwide, investigations from multiple perspectives and of various mechanisms of action are urgently required to increase the HBV cure rate. Targeting the encapsidation of the nuclear capsid protein (core protein, Hbc) has emerged as an attractive strategy for inhibiting the viral assembly process; however, a drug targeting this mechanism has not yet been approved. We synthesized novel sulfamoylbenzamides (SBAs) as capsid assembly modulators of HBV and found that the effects and safety profiles of compounds **3** and **8** have potential therapeutic applicability against HBV. The formation of tubular particles was time-dependent in the presence of **3**, indicating a new mode of protein assembly by SBA compounds. Our findings provide a new entity for developing safe and efficient treatments for HBV infection.

KEYWORDS: Hepatitis B virus, chronic hepatitis B infection, antiviral, capsid assembly modulator, sulfamoylbenzamide



EC ₅₀ (μM)	0.30 ± 0.15	0.29 ± 0.03
CC ₅₀ (μM)	16.0 ± 0.3	47.5 ± 0.5
SI	53.3	164.1

Hbc(1–149)-His assembly in the presence of **3**

Hepatitis B virus (HBV), a member of the *Hepadnaviridae* family, is an enveloped virus with a partial, circular DNA genome of ~3.2 kb in length. Because acute or chronic hepatitis B (CHB) infections in humans can potentially proceed to cirrhosis and hepatocellular carcinoma, it has become one of the greatest global health concerns, with reports of over 257 million infection cases and 887 000 deaths by HBV annually.¹

The currently approved anti-HBV agents for managing CHB include PEGylated interferon alpha and nucleos(t)ide analogues.^{2–4} However, the current drugs cannot completely cure this disease, and lifelong treatments result in serious side effects and the emergence of drug resistance.^{5,6} Moreover, an absolute cure for HBV infection has been regarded as unachievable, mainly because of the viral persistence reservoir, covalently closed circular DNA (cccDNA).^{7,8} As an episomal minichromosome, cccDNA serves as a stable replication template for the transcription of viral RNA in infected human hepatocytes. Therefore, along with inhibitors targeting cccDNA,^{9,10} different antiviral strategies, including the suppression of viral replication or the stimulation of the host immune response, have been introduced to control HBV infections.^{11–13}

In the exploration of promising antiviral targets among HBV proteins translated from mRNA transcripts, capsid protein (core protein, Hbc) has been identified to be key in the regulation of viral infectivity.^{14,15} Icosahedral capsid particles

are constructed by the assembly of 120 Hbc dimers around complexes of pregenomic RNA (pgRNA) and HBV DNA polymerase. It has been known that amino acids 1–149 within the full-length Hbc of 183 amino acids are critical for the self-assembly process. Because the assembly of Hbc strictly controls the replication of HBV, modulating or inhibiting encapsidation has emerged as an attractive antiviral target.^{16–18}

There are two classes of small-molecule-based compounds targeting Hbc (Figure 1).^{16–18} Class-I inhibitors, such as the heteroaryldihydropyrimidine (HAP) derivative, BAY 41-4109,¹⁹ promote Hbc assembly and mislead dimers into irregular and abnormal formulations of capsid particles. Class-II inhibitors such as phenylpropenamides and sulfamoylbenzamides (SBAs), represented by AT-130²⁰ and NVR 3-778,²¹ respectively, disrupt encapsidation of pgRNA, thus constructing genetically empty, capsid-like particles. Although studies to develop efficient capsid assembly modulators (CAMs) to treat HBV infections have led to the release of several candidates

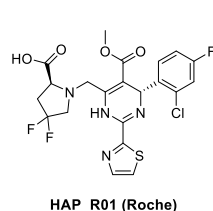
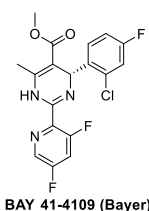
Received: November 19, 2020

Accepted: December 29, 2020

Published: February 2, 2021



• Class I inhibitors



• Class II inhibitors

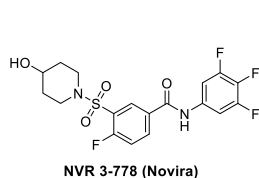
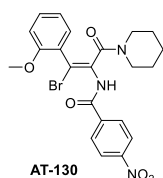


Figure 1. Representative capsid assembly modulators.

currently in clinical trials, the need for more efficient and safe compounds remains unmet.

Our prior efforts to improve anti-HBV activity starting from NVR 3-778 and HAP_R01 yielded a structurally related but more potent compound, KR-26556.²² Despite its cellular

potency evidenced by reduced HBV DNA levels in HepAD cells, the present findings in HepG2.2.15 cells (Table 1, entry 15, $EC_{50} = 0.27 \mu\text{M}$ and $CC_{50} = 19.7 \mu\text{M}$) revealed the need to develop more HBV-specific antiviral candidates. We aimed to synthesize more KR-26556 derivatives and identify alternative CAMs by investigating structure–antiviral activity relationships (SARs). We also explored the mode of protein assembly by transmission electron microscopy (TEM) to elucidate the undisclosed molecular mechanism of related compounds including KR-26556.

Table 1 shows that potency and selectivity values were higher for KR-26556 (15) than for NVR 3-778 (entries 15 and 16). This compound was found to be beneficial for maintaining both fluorine and amino groups in the central aromatic ring of 15. Therefore, we investigated the antiviral and cytotoxic effects of substituents in the A ring of KR-26556 for SAR studies (Figure 2).

Although the 3- or 4-fluoro derivatives, compounds 1 and 2, were not as potent as trifluoro 15 (entries 1 and 2 vs 15), the improved cell viability in the presence of 1 and 2 led to an examination of the effects of other substituents on potency and cytotoxicity. Antiviral activity was more potent for the 3,4-difluoro compound 3 than for monofluoro compounds (entry

Table 1. Structure–Activity Relationships of the A Ring

Entry	Structure	EC_{50} (μM) ^a	CC_{50} (μM) ^b	SI	Entry	Structure	EC_{50} (μM) ^a	CC_{50} (μM) ^b	SI
1		0.57 ± 0.07	45.8 ± 0.5	80.4	9		1.08 ± 0.28	>900	>833.3
2		0.83 ± 0.06	29.3 ± 3.4	35.3	10		>3.30	17.8 ± 1.7	n.d.
3		0.30 ± 0.15	16.0 ± 0.3	53.3	11		>3.30	30.1 ± 1.7	n.d.
4		0.83 ± 0.12	18.5 ± 2.5	22.3	12		>3.30	>900	n.d.
5		2.18 ± 0.03	20.3 ± 0.0	9.3	13		>3.30	5.9 ± 0.1	n.d.
6		2.07 ± 0.08	20.4 ± 3.7	9.9	14		>3.30	8.7 ± 0.2	n.d.
7		2.18 ± 0.11	47.3 ± 0.3	21.7	15		0.27 ± 0.02	19.7 ± 1.0	73.0
8		0.29 ± 0.03	47.5 ± 0.5	164.1	16	NVR 3-778	1.04 ± 0.01	8.6 ± 0.3	8.3

^aAntiviral effects of compounds. After 5 days of incubation with the compounds, HBV DNA was purified from the HepG2.2.15 cell culture supernatants and subjected to real-time PCR. ^bCytotoxicity of compounds determined by cell viability assays after incubating HepG2.2.15 cells with compounds. Data are shown as the mean \pm SD of three independent experiments. n.d.: not determined.

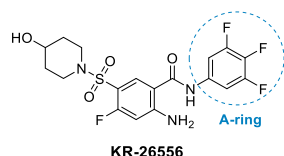


Figure 2. Structure of KR-26556 (**15**).

3 vs 1 and 2), with comparable EC_{50} and CC_{50} values as those of compound **15**.

In contrast, among chlorine-substituted compounds **4–6**, **5** and **6** had deleterious effects on both EC_{50} and selectivity index (SI) values (entries 5 and 6). Notably, the 3-chloro-4-fluoro compound **4** had better antiviral activity than compounds **5** and **6**, indicating the advantage of a *para*-fluoro group, which was also evident in the comparison of compounds **1** and **2**.

We investigated the different functionalities at the *meta*-position of the A ring while retaining the *para*-substituted fluoride (entries 7–9). Difluoromethyl-substituted compound **8** selectively and efficiently inhibited HBV, whereas the trifluoromethyl group of compound **7** did not enhance the EC_{50} and showed low antiviral selectivity (entries 7 and 8). Most noticeably, when the *meta*-position was replaced with a cyano group in compound **9**, cell cytotoxicity was lost ($CC_{50} > 900 \mu M$), despite having decreased antiviral potency compared with compound **8** (entry 9). Moreover, consistent with previous data, a similar series of compounds with chlorine at the *para*-position (entries 10 and 11) or 3-halo-4-trifluoro compounds (entries 13 and 14) lost their anti-HBV effects, and most were quite cytotoxic. Compound **12** had no cytotoxicity or antiviral effects (entry 12).

The SAR studies of the A ring revealed several features associated with potency and selectivity. Three fluorines, as in compound **15** and NVR 3-778, are not prerequisite for antiviral efficacy. We determined the importance of *para*-substituted fluorine atoms for the potent inhibition of HBV, which suggested the importance of incorporating substituents with appropriate size and polarity. In addition, *meta*-CN-substituted compounds **9** and **12** were essentially noncytotoxic, with the best SI for compound **9**. These findings support further optimization studies and provide insights that are useful for improving the current HBV CAMs in terms of the enhanced SI value.

The molecular docking studies with the HBV core protein (PDB code: 5T2P) showed that the proposed binding mode of **3** was similar to those of the cocrystallized ligand and **15** in our previous study (Figure 3).²² The oxygen of the benzamide in **3** forms a key hydrogen bond with Trp102 (B chain), whereas Thr128 (C chain) forms additional hydrogen bonds with the nitrogen of the benzamide group. In addition, the piperidyl group of **3** points toward the solvent-exposed area. The amino group of the central aromatic ring in **3** notably enabled the advantageous hydrogen bonding with Tyr118.²² Finally, the difluoro-substituted phenyl group of **3** bound to the hydrophobic pocket formed by Pro25, Leu30, Thr33, Ile105, and Ser106 of the B chain and Val124 of the C chain.

To assess the effect of the series of compounds on the capsid assembly, we purified the recombinant Hbc(1–149)-His protein for TEM analysis (Figure 4A). We initially tested whether this recombinant protein could self-assemble into nanosized spherical particles. We found that incubating Hbc(1–149)-His in assembly buffer for 5 days resulted in

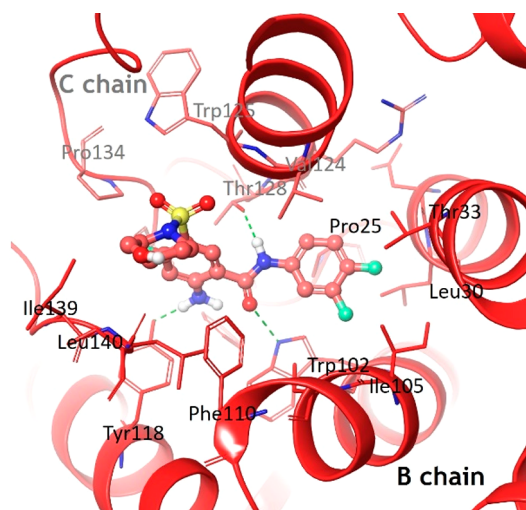


Figure 3. Predicted binding mode of compound **3** with the HBV core protein (PDB code: 5T2P). Red ribbons, B and C chains. Green dashed lines, hydrogen bonds. Key interaction residues are represented by stick models and labeled with three-letter amino acid codes for clarity.

the construction of spherical particles of 35.6 ± 2.6 nm in diameter (Figure 4B,C). Interestingly, the representative compound **3** facilitated the self-assembly of Hbc(1–149)-His into mainly spherical (~ 43 nm in diameter) and short rod-shaped particles (~ 100 nm in length) after incubation for 12 h (Figure 4D). Some particles had irregular or immature shapes with nicks. Further incubation of proteins with compound **3** for 3 or 5 days resulted in the generation of longer tubular particles, eventually becoming rod-shaped particles with lengths ranging from nanometers to micrometers (Figure 4E,F). These results suggest that the anti-HBV activity of compound **3** is due to the stimulation of aberrant Hbc particle formation.

Structurally, the compounds in Table 1 are typically class-II capsid assembly modulators, SBAs. However, the structures of capsid particles for class-II compounds reportedly produce only capsid-like spherical particles without the viral genome.²³ In contrast, the class-I capsid inhibitor, BAY 41-4109, has a unique tubular ensemble like compound **3**.²⁴ It is plausible that slight changes in the structures may result in different thermodynamic outcomes of capsid assembly. The different morphological consequences of the same SBA series of molecules indicated a need to explore the molecular mechanism of each compound to understand its exact mode of action.

To obtain further insight into the binding-derived outcomes in the course of dimer assembly, we predicted the conformational changes of unliganded/liganded AB dimers of Hbc through molecular dynamics (MD) simulations. Simulations at 50 ns revealed that the conformation considerably differed between the AB dimer structure and the unliganded X-ray crystal structure (Figure 5). Further analysis of the structural changes of AB dimers in the presence of bound BAY 41-4109, HAP_R01, and NVR 3-778 revealed distinctive changes in their dimeric conformations (Figure S12B–D). On the basis of the dynamics of the protein conformations determined by MD simulations, the apparent changes in the conformations of the AB dimer and the degree of α -helix flexibility induced by compound **3** possibly perturbed the original interactive angles

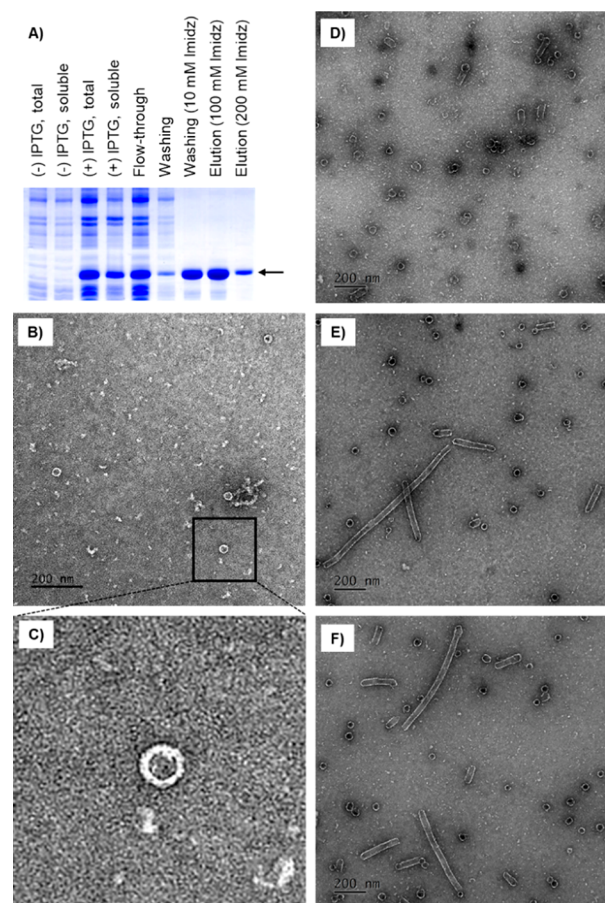


Figure 4. Effects of compound 3 on Hbc self-assembly. (A) Purification of His-tagged Hbc(1–149) protein. Total *E. coli* lysates or soluble fractions were prepared before (–) or after (+) isopropyl β -D-1-thiogalactopyranoside (IPTG) induction. Flow-through, wash, and eluted fractions of the sample on Ni-NTA columns were separated by SDS-PAGE. Imidz, imidazole. The Hbc(1–149)-His protein is marked with an arrow on the right side of the Coomassie blue-stained gel. (B–F) TEM analysis. (B) Hbc(1–149)-His protein (150 μ M) incubated without compounds at 4 $^{\circ}$ C for 5 days. (C) Rectangle area in panel B. Hbc(1–149)-His protein (150 μ M) incubated with compound 3 (30 μ M) for (D) 12 h, (E) 3 days, and (F) 5 days. Scale bar, 200 nm.

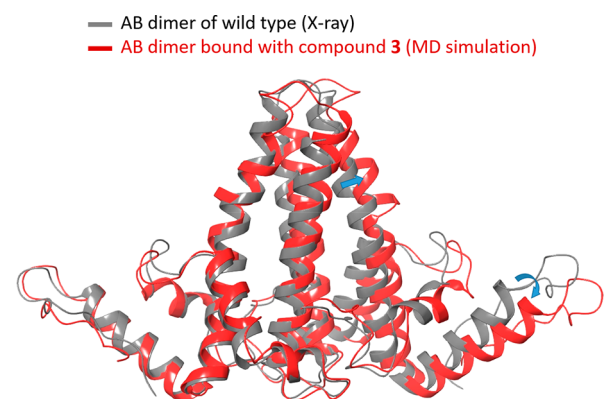


Figure 5. Structural comparison of AB dimers. Overlays of the AB dimer bound to compound 3 on molecular dynamics simulation with the X-ray crystal structure for Hbc alone.

between monomers, eventually triggering the atypical assembly of viral capsid particles.

We pharmacologically assessed the active compounds 3 and 8 based primarily on their anti-HBV activity (EC_{50} of ~ 0.3 μ M) *in vitro* and secondarily on the selectivity (SI > 50). Table 2 summarizes the results. Both compounds only minimally

Table 2. Safety and Pharmacokinetic Profile of Compounds 3 and 8 *In Vitro*

	3	8
CYP inhibition (IC_{50} , μ M) ^a		
1A2	>100.0	45.5
2C9	25.0	25.2
2C19	18.3	19.0
2D6	29.3	26.7
3A4	41.0	20.8
cardiotoxicity (IC_{50} , μ M)		
hERG ligand binding assay	50.0	>10
liver microsomal phase-I stability ^b		
rat (%)	67.9 \pm 0.4	54.1 \pm 2.3
human (%)	68.1 \pm 2.5	40.5 \pm 3.2
rat ($t_{1/2}$, min)	52.0 \pm 2.2	29.3 \pm 0.7
human ($t_{1/2}$, min)	74.4 \pm 4.5	30.6 \pm 0.8
plasma stability ^c		
rat (%)	84.6 \pm 2.6	99.6 \pm 6.0
human (%)	93.6 \pm 4.2	100.0 \pm 11.1
plasma protein binding ^d		
rat (%)	92.7 \pm 2.6	89.2 \pm 2.7
human (%)	96.5 \pm 1.2	97.1 \pm 0.6

^a IC_{50} (μ M) in human liver microsomes determined using cocktail substrate assays. ^bLiver microsomal phase-I stability (% remaining after 30 min). ^cRatio (%) remaining after 4 h of incubation at 37 $^{\circ}$ C. ^dPlasma protein binding rate (%). Assay conditions are described in the Supporting Information. All data are shown as the mean \pm SD; $n = 3$ for all.

inhibited the metabolic activity of cytochrome P450 (CYP) with $IC_{50} > 10$ μ M against five major CYP isozymes (CYP1A2, CYP2C9, CYP2C19, CYP2D6, and CYP3A4) but did not significantly bind to hERG ($IC_{50} > 10$ μ M), indicating that both compounds were minimally hepatotoxic or cardiotoxic at their antiviral concentrations. In addition, liver microsomal stability tests showed that 67.9 and 68.1% of compound 3 remained without degradation, resulting in half lives of 52.0 and 74.4 min in rat and human liver microsomes, respectively. In contrast, only 54.1 and 40.5% of compound 8 was intact with shorter half lives (29.3 and 30.6 min in rat and human microsomes, respectively), clearly emphasizing the metabolic instability of compound 8 compared with compound 3. Additionally, both compounds were stable in rat and human plasma. Compounds 3 (84.6 and 93.6%) and 8 (99.6 and 100.0%) were detected even after 4 h of incubation at 37 $^{\circ}$ C. The protein binding analysis showed that the bound fraction of compound 3 was 92.7% in rat plasma and 96.5% in human plasma, whereas compound 8 gave 89.2 and 97.1%, respectively.

To clarify the pharmacokinetic (PK) properties of compounds 3 and 8 *in vivo*, the time courses of plasma concentrations of the two compounds were assessed in male Sprague–Dawley (SD) rats, and Table 3 summarizes the results. After intravenous (I.V.) administration, the plasma clearance of compound 3 was moderate at 2.1 L/h/kg with a volume distribution of 2.9 L/kg. The mean terminal half life and area under the plasma concentration–time curve from

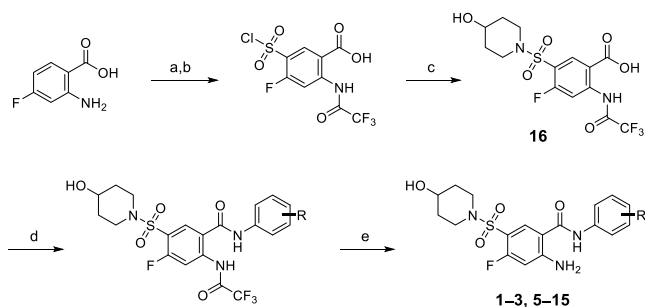
Table 3. *In Vivo* Pharmacokinetic Parameters of Compounds 3 and 8 in SD Male Rats^a

parameter ^b	3		8	
	I.V. (5 mg/kg) ^c	P.O. (5 mg/kg) ^d	I.V. (5 mg/kg) ^c	P.O. (5 mg/kg) ^d
T_{max} (h)	N/A	1.67 ± 2.02	N/A	1.33 ± 0.58
C_{max} (μg/mL)	N/A	0.48 ± 0.39	N/A	0.28 ± 0.15
$T_{1/2}$ (h)	1.22 ± 0.07	3.84 ± 0.20	2.55 ± 0.33	5.16 ± 1.16
AUC_{last} (μg·h/mL)	2.45 ± 0.51	2.08 ± 0.33	2.31 ± 0.15	1.15 ± 0.53
AUC_{∞} (μg·h/mL)	2.50 ± 0.48	2.10 ± 0.32	2.33 ± 0.15	1.23 ± 0.57
CL (L/h/kg)	2.05 ± 0.40	N/A	2.16 ± 0.14	N/A
V_{ss} (L/kg)	2.88 ± 0.85	N/A	3.59 ± 0.82	N/A
F_l (%)	N/A	84.17	N/A	49.94

^aDetailed pharmacokinetics of compounds 3 and 8 are described in Supporting Information. ^bValues are shown as the mean ± standard deviation of at least three independent experiments. ^cParameters from intravenous administration. ^dParameters from oral administration.

time zero to infinity (AUC_{∞}) of compound 3 were 1.2 h and 2.5 μg·h/mL, respectively. The clearances of compound 8 (2.2 L/h/kg) and AUC_{∞} (2.3 μg·h/mL) were similar to those of compound 3, in contrast with the higher volume of distribution (3.6 L/kg) and the longer half life (2.6 h). When compound 3 (5 mg/kg) was administered orally (P.O.), the maximum concentration (C_{max}) was 0.48 μg/mL, and the level of exposure (AUC_{∞}) was 2.10 μg·h/mL, which afforded a high oral bioavailability of 84.2%. In contrast, the estimated oral bioavailability of compound 8 was moderate at 49.9%, corresponding more to the lower C_{max} (0.28 μg/mL) and AUC_{∞} (1.23 μg·h/mL) compared with compound 3.

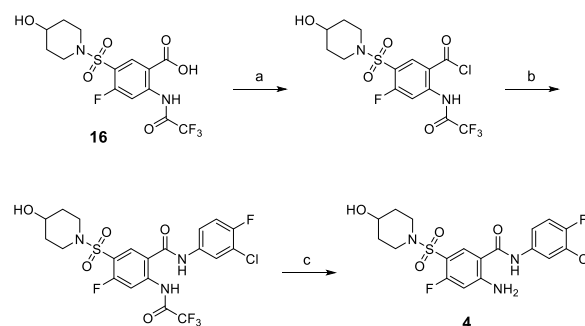
Scheme 1 summarizes the synthesis of compounds 1–3 and 5–14 initiated with amine protection. Chlorosulfonylation at

Scheme 1. Synthetic Route for Compounds 1–3 and 5–15^a

^aReagents and conditions: (a) trifluoroacetic anhydride, CH_2Cl_2 , 0–25 °C, 10 h (93%); (b) $ClSO_3H$, 0–170 °C, 72 h; (c) piperidin-4-ol, DIPEA, dioxane/ H_2O (10:1), 25 °C, 2 h (34%, two-step yield); (d) HATU, DIPEA, amine, DMF, 25–60 °C, 12–36 h; (e) 1 N NaOH (aq.), MeOH, 25 °C, 2 h (4–32%, two-step yield).

position C5 was accomplished by incubation with chlorosulfonic acid at 170 °C for 72 h. The resulting carboxylic acid with a chlorosulfonyl group at C5 was further reacted with piperidin-4-ol. Amide intermediates were obtained via coupling of acid 16 with various amines using 1-[bis(dimethylamino)methylene]-1*H*-1,2,3-triazolo[4,5-*b*]pyridinium 3-oxide hexafluorophosphate (HATU) and *N,N*-diisopropylethylamine (DIPEA) in dimethylformamide (DMF). Finally, aqueous 1 N NaOH was added in excess amounts to obtain the desired product.

Compound 4 was synthesized according to Scheme 2 but with an additional step to prepare the amide. To obtain the acid chloride intermediate, thionyl chloride was heated with carboxylic acid 16 at 80 °C for 2 h. Amine was added to the

Scheme 2. Synthetic Route for Compound 4^a

^aReagents and conditions: (a) $SOCl_2$, 80 °C, 2 h; (b) 3-chloro-4-fluoroaniline, DIPEA, THF, 25 °C, 15 h (20%, two-step yield); (c) 1 N NaOH (aq.), 25 °C, 2 h (24%).

resulting acid chloride in tetrahydrofuran (THF) to generate the desired amide bond.

In summary, we developed new HBV capsid assembly modulators, compounds 3 and 8, and then evaluated their anti-HBV potency (EC_{50}), selectivity (SI) *in vitro*, and pharmacokinetics (PK) *in vitro* and *in vivo*. The findings showed that both compounds specifically inhibited HBV replication with validated PK properties. The mode of action of compound 3 showed the time-dependent formation of tubular particles, and computational studies sequentially revealed the origins of this phenomenon. However, the detailed mechanism of abnormal assembly triggered by compound 3 remains elusive because of the high complexity during the assembly process. Our results provide insight into pathways requiring further study and develop novel capsid assembly modulators with the desired potency and safety.

■ ASSOCIATED CONTENT

Supporting Information

The Supporting Information is available free of charge at <https://pubs.acs.org/doi/10.1021/acsmchemlett.0c00606>.

Experimental procedures for biological assays, ligand docking studies, molecular dynamics simulations, and synthetic procedures and characterization data for presented compounds, including the spectral copies of 1H and ^{13}C NMR spectra (PDF)

AUTHOR INFORMATION

Corresponding Authors

Hyejin Kim – Therapeutics & Biotechnology Division, Korea Research Institute of Chemical Technology, Daejeon 34114, Republic of Korea; orcid.org/0000-0002-6797-2360; Phone: +82-42-860-7130; Email: hjinkim@krikt.re.kr; Fax: +82-42-860-7160

Soo Bong Han – Therapeutics & Biotechnology Division, Korea Research Institute of Chemical Technology, Daejeon 34114, Republic of Korea; Department of Medicinal Chemistry and Pharmacology, University of Science & Technology, Daejeon 34113, Republic of Korea; orcid.org/0000-0002-7831-1832; Phone: +82-42-860-7133; Email: sbhan@krikt.re.kr; Fax: +82-42-860-7160

Authors

Yeon Hee Lee – Therapeutics & Biotechnology Division, Korea Research Institute of Chemical Technology, Daejeon 34114, Republic of Korea; Department of Medicinal Chemistry and Pharmacology, University of Science & Technology, Daejeon 34113, Republic of Korea

Hyeon-Min Cha – Therapeutics & Biotechnology Division, Korea Research Institute of Chemical Technology, Daejeon 34114, Republic of Korea; Graduate School of New Drug Discovery and Development, Chungnam National University, Daejeon 34134, Republic of Korea

Jun Yeon Hwang – Therapeutics & Biotechnology Division, Korea Research Institute of Chemical Technology, Daejeon 34114, Republic of Korea

So Yeong Park – Therapeutics & Biotechnology Division, Korea Research Institute of Chemical Technology, Daejeon 34114, Republic of Korea; Department of Medicinal Chemistry and Pharmacology, University of Science & Technology, Daejeon 34113, Republic of Korea

Avinash G. Vishakantegowda – Therapeutics & Biotechnology Division, Korea Research Institute of Chemical Technology, Daejeon 34114, Republic of Korea; Department of Medicinal Chemistry and Pharmacology, University of Science & Technology, Daejeon 34113, Republic of Korea; orcid.org/0000-0003-0712-6418

Ali Imran – Therapeutics & Biotechnology Division, Korea Research Institute of Chemical Technology, Daejeon 34114, Republic of Korea

Joo-Youn Lee – Therapeutics & Biotechnology Division, Korea Research Institute of Chemical Technology, Daejeon 34114, Republic of Korea

Yoon-Sun Yi – Center for Research Equipment, Korea Basic Science Institute, Cheongju 28119, Republic of Korea

Sangmi Jun – Center for Research Equipment, Korea Basic Science Institute, Cheongju 28119, Republic of Korea

Ga Hyeon Kim – School of Pharmacy, Sungkyunkwan University, Suwon 16419, Republic of Korea; AbTis Co. Ltd. Suwon Venture Valley II, Suwon 16648, Republic of Korea; orcid.org/0000-0002-8535-3969

Hyo Jin Kang – AbTis Co. Ltd. Suwon Venture Valley II, Suwon 16648, Republic of Korea

Sang J. Chung – School of Pharmacy, Sungkyunkwan University, Suwon 16419, Republic of Korea; AbTis Co. Ltd. Suwon Venture Valley II, Suwon 16648, Republic of Korea; orcid.org/0000-0002-3501-212X

Meehyein Kim – Therapeutics & Biotechnology Division, Korea Research Institute of Chemical Technology, Daejeon 34114, Republic of Korea; Graduate School of New Drug

Discovery and Development, Chungnam National University, Daejeon 34134, Republic of Korea

Complete contact information is available at: <https://pubs.acs.org/10.1021/acsmchemlett.0c00606>

Author Contributions

Y.H.L. and H.-M.C. contributed equally.

Notes

The authors declare no competing financial interest.

ACKNOWLEDGMENTS

This study was supported by the Korea Research Institute of Chemical Technology (grant no. KK2032-00).

ABBREVIATIONS

AUC_{last} ($\mu\text{g}\cdot\text{h}/\text{mL}$), area under the plasma concentration–time curve from time zero to time of last measurable concentration; AUC_∞ ($\mu\text{g}\cdot\text{h}/\text{mL}$), area under the plasma concentration–time curve from time zero to time infinity; F_t (%), bioavailability; CL (L/h/kg), total clearance from plasma; I.V., intravenous; P.O., per os; T_{max} (h), time of maximum drug concentration; C_{max} (mg/mL), maximum plasma concentration; T_{1/2} (h), terminal half life; V_{ss} (L/kg), steady-state volume of distribution

REFERENCES

- (1) World Health Organization Hepatitis B fact sheet, 2020. <https://www.who.int/news-room/fact-sheets/detail/hepatitis-B> (accessed July 10, 2020).
- (2) Yuen, M. F.; Lai, C. L. Treatment of chronic hepatitis B: Evolution over two decades. *J. Gastroenterol. Hepatol.* **2011**, *26*, 138–143.
- (3) Fung, J.; Lai, C. L.; Seto, W. K.; Yuen, M. F. Nucleoside/nucleotide analogues in the treatment of chronic hepatitis B. *J. Antimicrob. Chemother.* **2011**, *66*, 2715–2725.
- (4) Craxi, A.; Cooksley, W. G. Pegylated interferons for chronic hepatitis B. *Antiviral Res.* **2003**, *60*, 87–89.
- (5) Shaw, T.; Bartholomeusz, A.; Locarnini, S. HBV drug resistance: Mechanisms, detection and interpretation. *J. Hepatol.* **2006**, *44*, 593–606.
- (6) Zoulim, F.; Locarnini, S. Hepatitis B Virus Resistance to Nucleos(t)ide Analogues. *Gastroenterology* **2009**, *137*, 1593–1608.
- (7) Nassal, M. HBV cccDNA: viral persistence reservoir and key obstacle for a cure of chronic hepatitis B. *Gut* **2015**, *64*, 1972–1984.
- (8) Allweiss, L.; Dandri, M. The Role of cccDNA in HBV Maintenance. *Viruses* **2017**, *9*, 156.
- (9) Zhu, A.; Liao, X.; Li, S.; Zhao, H.; Chen, L.; Xu, M.; Duan, X. HBV cccDNA and Its Potential as a Therapeutic Target. *JCTH* **2019**, *7*, 258–262.
- (10) Ligat, G.; Goto, K.; Verrier, E.; Baumert, T. F. Targeting Viral cccDNA for Cure of Chronic Hepatitis B. *Current Hepatology Reports* **2020**, *19* (3), 235–244.
- (11) Liang, T. J.; Block, T. M.; McMahon, B. J.; Ghany, M. G.; Urban, S.; Guo, J.-T.; Locarnini, S.; Zoulim, F.; Chang, K.-M.; Lok, A. S. Present and future therapies of hepatitis B: From discovery to cure. *Hepatology* **2015**, *62*, 1893–1908.
- (12) Dawood, A.; Abdul Basit, S.; Jayaraj, M.; Gish, R. G. Drugs in Development for Hepatitis B. *Drugs* **2017**, *77* (12), 1263–1280.
- (13) Lopatin, U. Drugs in the Pipeline for HBV. *Clin. Liver Dis.* **2019**, *23* (3), 535–555.
- (14) Zlotnick, A.; Venkatakrishnan, B.; Tan, Z.; Lewellyn, E.; Turner, W.; Francis, S. Core protein: A pleiotropic keystone in the HBV lifecycle. *Antiviral Res.* **2015**, *121*, 82–93.
- (15) Diab, A.; Foca, A.; Zoulim, F.; Durantel, D.; Andrisani, O. The diverse functions of the hepatitis B core/capsid protein (HBc) in the

viral life cycle: Implications for the development of HBc-targeting antivirals. *Antiviral Res.* **2018**, *149*, 211–220.

(16) Feng, S.; Gao, L.; Han, X.; Hu, T.; Hu, Y.; Liu, H.; Thomas, A. W.; Yan, Z.; Yang, S.; Young, J. A. T.; Yun, H.; Zhu, W.; Shen, H. C. Discovery of Small Molecule Therapeutics for Treatment of Chronic HBV Infection. *ACS Infect. Dis.* **2018**, *4* (3), 257–277.

(17) Yang, L.; Liu, F.; Tong, X.; Hoffmann, D.; Zuo, J.; Lu, M. Treatment of Chronic Hepatitis B Virus Infection Using Small Molecule Modulators of Nucleocapsid Assembly: Recent Advances and Perspectives. *ACS Infect. Dis.* **2019**, *5*, 713–724.

(18) Nijampatnam, B.; Liotta, D. C. Recent advances in the development of HBV capsid assembly modulators. *Curr. Opin. Chem. Biol.* **2019**, *50*, 73–79.

(19) Deres, K.; Schröder, C. H.; Paessens, A.; Goldmann, S.; Hacker, H. J.; Weber, O.; Krämer, T.; Niewöhner, U.; Pleiss, U.; Stoltefuss, J.; Graef, E.; Koletzki, D.; Masantschek, R. N. A.; Reimann, A.; Jaeger, R.; Groß, R.; Beckermann, B.; Schlemmer, K.-H.; Haebich, D.; Rübsamen-Waigmann, H. Inhibition of hepatitis B virus replication by drug-induced depletion of nucleocapsids. *Science* **2003**, *299*, 893–896.

(20) Delaney, W. E.; Edwards, R.; Colledge, D.; Shaw, T.; Furman, P.; Painter, G.; Locarnini, S. Phenylpropenamide derivatives AT-61 and AT-130 inhibit replication of wild-type and lamivudine-resistant strains of hepatitis B virus in vitro. *Antimicrob. Agents Chemother.* **2002**, *46*, 3057–3060.

(21) Gane, E.; Schwabe, C.; Walker, K.; Flores, L.; Hartman, G.; Klumpp, K.; Liaw, S.; Brown, N. Phase 1a safety and pharmacokinetics of NVR 3-778, a potential first-in-class HBV core inhibitor. *Hepatology* **2014**, *60*, 1279A.

(22) Na, H. G.; Imran, A.; Kim, K.; Han, H. S.; Lee, Y. J.; Kim, M.-J.; Yun, C.-S.; Jung, Y.-S.; Lee, J.-Y.; Han, S. B. Discovery of a New Sulfonamide Hepatitis B Capsid Assembly Modulator. *ACS Med. Chem. Lett.* **2020**, *11*, 166–171.

(23) Zhou, Z.; Hu, T.; Zhou, X.; Wildum, S.; Garcia-Alcalde, F.; Xu, Z.; Wu, D.; Mao, Y.; Tian, X.; Zhou, Y.; Shen, F.; Zhang, Z.; Tang, G.; Najera, I.; Yang, G.; Shen, H. C.; Young, J. A. T.; Qin, N. Heteroaryldihydropyrimidine (HAP) and Sulfamoylbenzamide (SBA) Inhibit Hepatitis B Virus Replication by Different Molecular Mechanisms. *Sci. Rep.* **2017**, *7*, 42374.

(24) Liu, C.; Fan, G.; Wang, Z.; Chen, H. S.; Yin, C. C. Allosteric conformational changes of human HBV core protein transform its assembly. *Sci. Rep.* **2017**, *7*, 1404.